Temperature effect on the electrical properties of chromium oxide (Cr_2O_3) thin films

MD. JULKARNAIN, J. HOSSAIN, K. S. SHARIF, K. A. KHAN[*]
Department of Applied Physics and Electronic Engineering, University of Rajshahi, Rajshahi-6205, Bangladesh

Chromium Oxide (Cr_2O_3) thin films have been prepared by thermal evaporation onto glass substrate at a pressure of about 6×10^{-4} Pa. Structural and compositional analysis has been carried out by XRD, SEM and EDAX method. The heating and cooling cycles of the samples are reversible in the investigated temperature range after successive heat-treatment in air. Temperature dependence of electrical conductivity shows a semiconducting behavior. The thickness dependence of conductivity is well in conformity with the Fuchs-Sondheimar theory. The Hall coefficient shows a positive sign exhibiting p-type carriers. Optical study has been employed to determine the band gap of the samples.

1. Introduction

Research and development on thin films have led to the conclusion that different classes of materials are of particular interest for different applications. The Cr_2O_3 thin films are of great interest due to their wide variety of technological applications. This oxide exhibit high hardness and high wear with corrosion resistance which are important properties for protective coating applications [1], it has already found several applications as protective coatings on read–write heads in digital magnetic recording units [2] and in gas-bearing applications. It has been studied for optical and electronic uses such as selectively absorbing films for solar energy conversion [3], solar energy shielding films for windows [4], and electrode material for electrochromic windows [5]. The Cr_2O_3 have been extensively studied as potential cathode material for lithium batteries [6]. Currently, low-reflective Cr_2O_3/Cr films are widely used as black matrix films in liquid crystal displays [7]. Literature reports indicate that thin films of Cr_2O_3 have been produced by a number of techniques by a number of researchers. These include the vacuum evaporation [8], sputtering [1,2,9], CVD method [7, 10-13], Spray pyrolysis [14] and reactive pulsed laser ablation techniques [15].   In this paper, we report on structural and temperature effect on the electrical properties of Cr_2O_3 thin films obtained by thermal evaporation techniques.

2. Experimental

Chromium Oxide (Cr_2O_3) films have been deposited onto glass substrate from Cr powder (99.999% pure) obtained from Goodfellow Chemical Company, England, by thermal evaporation method using an EDWARDS E 306A vacuum coating unit at a pressure of about 6×10^{-4} Pa. Before deposition, the deposition chamber has been thoroughly cleaned with emery paper and cotton wool by wetting acetone and then dried with a dryer. A small quantity of source materials have been placed on the clean Tungsten boat shaped source. The glass substrates have been then first cleaned in chromic acid solution and then washed in distilled water. After washing and drying in hot air, substrates has been then again cleaned in acetone and dried in hot air, and then used for deposition. Well shaped mask have been placed on substrate on which film should be grown and the substrate-mask couple have been clamped with the holder about 6 cm apart from the source and the chamber bell-jar is placed on the base plate. When required vacuum is obtained, the source is heated by (L. T. Power supply) passing current of about 92 A through the boat. A shutter is placed between the source and the substrate and it is removed when the evaporation of Cr seem to be uniform. The Cr film may oxidize in coating unit or open air after the film has been drawn from the chamber and form Cr_2O_3 by reaction with ambient Oxygen molecule. To make oxidization stable, the as-deposited thin films have been annealed in open air for about 3 hours at a temperature of 570 K. The thickness of the film has been measured by the Tolansky interference method with an accuracy of ± 5 nm [16].

Structural analysis of Cr_2O_3 thin films has been carried out in a PHYLIPS PW-3040 X' Pert PRO XRD System using the monochromatic CuKα radiation. Peak intensities have been recorded corresponding to 2θ values. Study of Scanning Electron Microscopy (SEM) and Energy Dispersive Analysis of X-ray (EDAX) has been carried out in a HITACHI S-3400N (SEM) System.

3. Results and discussion

3.1. Structural and compositional studies

Structural analysis of the as-deposited and annealed Cr_2O_3 thin films of different thicknesses (140-300nm), respectively, has been examined by X-ray Diffraction (XRD) technique. Fig. 1 shows the X-ray diffractograms of the annealed Cr_2O_3 thin films of different thickness. It is seen that there is only one peak in all three spectra, besides this, there is no noticeable peak in the entire range. It indicates that the films are amorphous in nature.
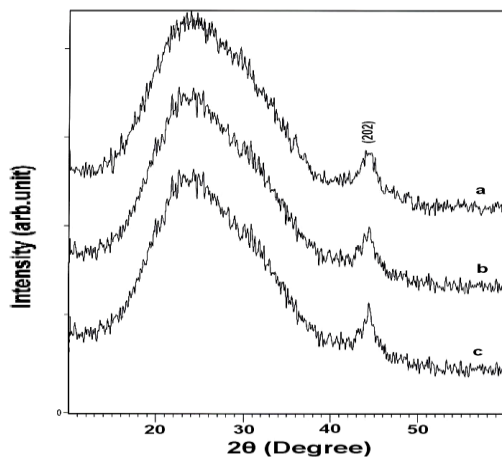

Fig. 1 X-ray diffractograms of the annealed Cr_2O_3 thin films, (a) for 140 nm, (b) for 240 nm and (c) for 300 nm.

SEM micrographs of the annealed Cr_2O_3 thin films of thickness 140 nm is shown in Fig. 2 and it exhibits almost smooth and uniform surface.
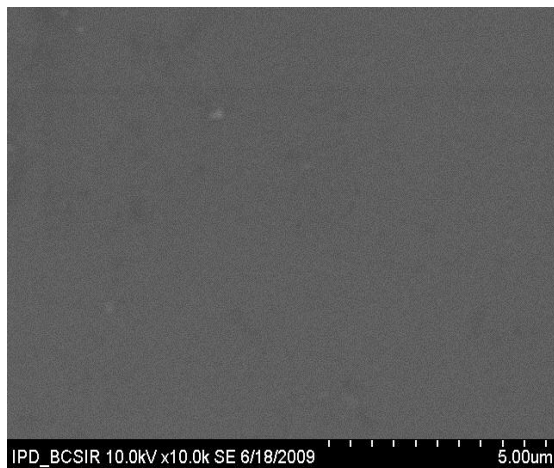

Fig. 2 SEM image of the annealed Cr_2O_3 thin film of thickness 140 nm.

The analysis of the elemental compositions for the Cr_2O_3 thin films of various thicknesses has been estimated by using the method of Energy Dispersive Analysis of X-ray (EDAX). The result of EDAX study shows a non-stoichiometric with oxygen deficient Cr_2O_3 thin film. The result of elemental compositions is shown in Table 1.

Table 1. Elemental composition of Cr_2O_3 thin film of variable thickness.

Status	Thickness	Cr (wt %)	O (wt %)
As-deposited	300	79.56	20.44
Annealed	140	73.48	26.52
	240	74.96	25.04
	300	75.12	24.88

3.2. Effect of heat treatment

The variation of resistivity with temperature for the as-deposited Cr_2O_3 thin film of thickness 140 nm is shown in Fig. 3. As shown in figure, the heating and cooling cycles are almost reversible after 4 cycle of operations in the investigated temperature range. The heating and cooling rate has so manually been maintained that it keeps a 4 K/min for each operation with a 10 minutes of time interval in between the cycles.
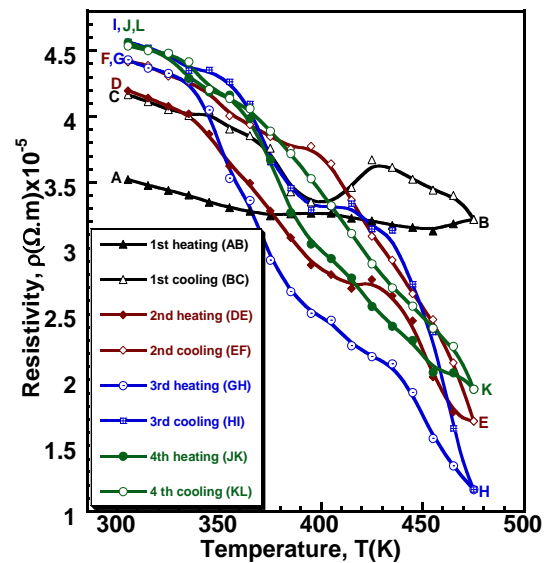

Fig. 3 The variation of resistivity vs. temperature of the as-deposited Cr_2O_3 thin film of thickness 140 nm.

During the first step of the heat treatment, the sample shows a small variation in resistivity in the investigated temperature range. In Fig. 3, AB shows the first heating cycle and BC represents the first cooling cycle in air. In first cooling cycle it is observed that the resistivity increases with decreasing temperature and shows an anomalous behavior between temperature 370 and 420 K. In first cooling cycle, the resistivity shows slightly an upward tendency and at room temperature difference in resistivity between first heating and first cooling cycle can be identified as AC. A tiny change in resistivity is observed at 10 minutes of time interval in between the cooling of first and heating of second cycle which is identified as CD. In the second step of heat-treatment in air, the heating cycle is shown by DE, which shows that the resistivity gradually falls with temperature in the

investigated temperature range and the falling rate of second heating cycle is greater than that of first cycle. The second cooling cycle is shown by EF, the resistivity increases with decreasing temperature but does not follow the heating cycle. The variation of resistivity in between second heating and second cooling cycle can be identified as DF and it is seen from the figure that DF is smaller than AC.

The third step of heat-treatment has been subsequently carried out in air. There is a very small variation in resistivity at 10 minutes of time interval in between the cooling of second and heating of third cycle. GH represents the variation of resistivity during the third heating cycle. It is clear from the figure that the resistivity gradually decreases with increasing temperature and the decreasing rate is greater the earlier one. The cooling cycle HI, again shows the increase in resistivity with decreasing temperature but it does not follow the heating cycle. Finally, after 10 minutes of wait, the resistivity does not change and it becomes stable. The point I or J represent the stable point of resistivity. JK represent the variation of resistivity of the fourth heating cycle in air. The reverse cooling cycle is identified as KL. The figure reveals that as the temperature decreases the third cooling cycle HI, fourth heating cycle JK and fourth cooling cycle KL are overlapped each other. It is also observed from figure that the difference between the fourth heating and fourth cooling cycles is small in the entire investigated range of temperature. Therefore the experiment shows that after 3-4 series of successive heating and cooling operation, the temperature dependence of electrical resistivity of Cr₂O₃ thin films becomes almost reversible.

During the first heating cycle in the open air oxygen molecule are chemisorbed at the grain boundaries and on the surface of the film which also reported by other researchers [17, 18]. It may be mentioned that the sample Cr₂O₃ has been produced by the oxidization of Cr thin film in air. The resistivity of author's sample at room temperature is $\sim 10^{-5}$ (Ω.m) and it may be noted that similar results $\sim 10^{-4}$ (Ω.m) have already been reported by other workers [19].

3.3. Electrical properties

Electrical conductivity σ has been measured as a function of temperature T in the 300–470 K range for the as-deposited and annealed films. The conductivity has been obtained by applying a d.c 5 V bias across the films with silver contact and recording the current and voltage simultaneously by using a standard four-probe van-der-Pauw technique [20].
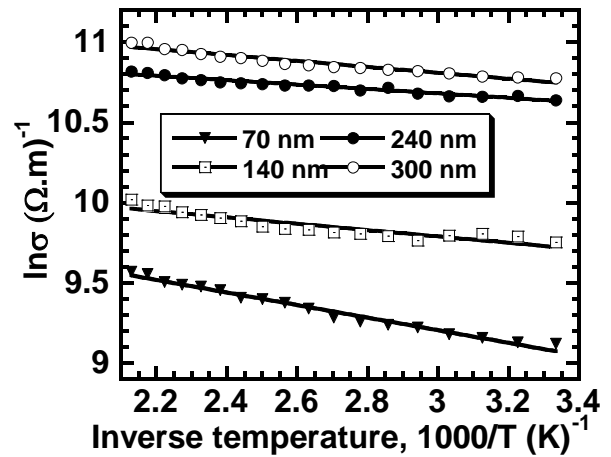

Fig. 4 Variation of lnσ vs. inverse temperature for the annealed Cr₂O₃ thin films of variable thickness.

Fig. 4 reports *lnσ vs. 1/T* curves for the annealed Cr₂O₃ samples of thickness 70, 140, 240 and 300 nm, respectively. It is seen that the conductivity increases with temperature indicating semiconducting behavior. The activation energies of these samples are calculated from the local gradients of *lnσ vs. 1/T* plots based on the following equation

$$\sigma = \sigma_0 \, exp(-\Delta E / 2\kappa_B T) \qquad (1)$$

where ΔE is the activation energy, σ_0 is a constant and K_B = Boltzmann constant, respectively. From this plots, the activation energy for four Cr₂O₃ samples of different thickness are calculated and shown in Table 2. From Table 2 it is seen that the activation energies of four samples is fairly low and is the order of 0.029-0.065 eV. The increase of activation energy with deceasing film thickness can be understood from the island structure theory based on tunneling of charged carriers between islands separated by short distance [21].

Table 2. Activation energies evaluated for the annealed Cr₂O₃ thin films.

Thickness (nm)	Activation energy (eV)
70	0.0650
140	0.0349
240	0.0309
300	0.0286

3.4. Size effect

The variation of electrical conductivity ($ln\sigma$) with thickness (*t*) for Cr_2O_3 thin films is shown in Fig. 5. It is seen from the figure that the conductivity increases with thickness and it attains a constant value $\approx 4.5 \times 10^4$ $(\Omega\text{-m})^{-1}$ at 240 nm.

Since the conductivity does not depend on the film thickness from 240 to 550 nm, the current density should be uniform and, therefore, the calculated conductivity are considered to give the volume conductivity, but not the surface conductivity in this thickness range. The thickness dependence of conductivity is well in conformity with the Fuchs-Sondheimer theory [22, 23]. The conductivity decreases below 240nm, which is probably due to discontinuous structure of the film.
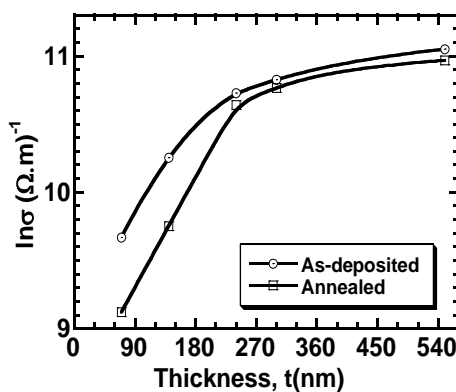

Fig. 5 Variation of conductivity vs. film thickness for the Cr_2O_3 thin films.

3.5. Hall study

The variation of Hall coefficient with temperature for the as-deposited Cr_2O_3 thin films of different thicknesses is shown in Fig. 6.
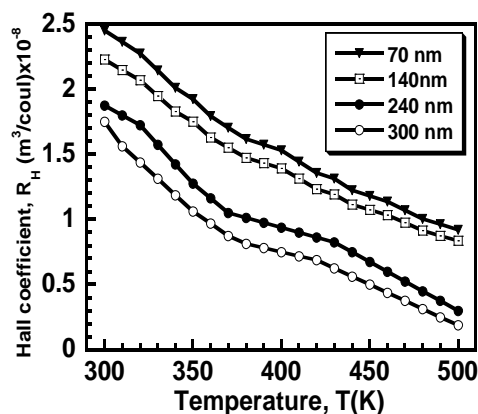

Fig. 6 Variation of Hall coefficient vs. temperature for the as-deposited Cr_2O_3 films of different thicknesses.

The Hall coefficient shows a positive sign exhibiting p-type carriers. From the figure it is seen that the Hall coefficient decreases with increasing temperature. The temperature dependent carrier concentration also studied for the as-deposited Cr_2O_3 thin films of different thicknesses and it is seen that the carrier concentration increases with increasing temperature. In the p-type semiconductor the acceptors which are ionized by thermal agitation released holes into the valance band [24]. As the temperature increases, more and more holes are released to the valance band. Hence the carrier concentration is increased with temperature. The carrier concentration of the samples varies from 2.55×10^{26} to 2×10^{27} m^{-3} in the investigated temperature range.

3.6. Thermoelectric power

The thermoelectric power measurements of as-deposited Cr_2O_3 thin films has been carried out by the integral method [25] in the temperature range 300 to 473K, respectively by taking pure metallic silver (Ag) as a reference metal. Fig. 7 shows the variation of thermo e.m.f. at different temperatures for four samples of thicknesses 70, 140, 190 and 240 nm, respectively. From the variation of thermo e.m.f vs. temperature, it is seen that the thermo e.m.f increases linearly with increasing temperature. The positive sign of the thermo e.m.f. indicates that the current carriers of the Cr_2O_3 thin films are holes and the films are p-type semiconductor which is well agreed with the Hall study.
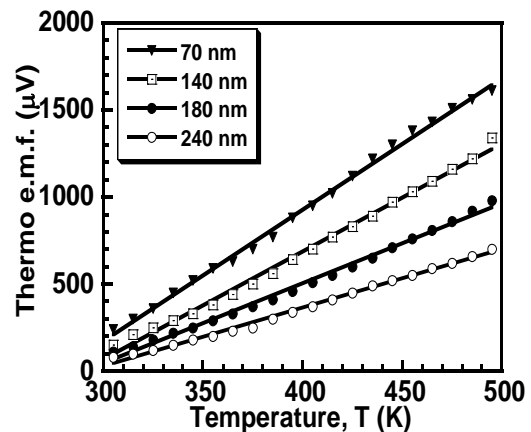

Fig. 7 Variation of thermo e.m.f vs. temperature for the as-deposited Cr_2O_3 thin films of different thicknesses.

4. Optical studies

Spectral transmittance T (λ) and near normal reflectance R (λ) of Cr_2O_3 thin films were measured at wavelength $0.3 < \lambda < 1.1$ μm using UV-Visible SHIMADZU double beam spectrophotometer. Fig. 8 shows the spectral transmittance/reflectance vs. wavelength spectra for a 70nm thick annealed thin film. Ii is seen that transmittance curve exhibits an appreciable order of transmittance in the visible as well as in the near infra-red region. The reflectance spectrum, however, shows a moderate value in the entire wavelength region.
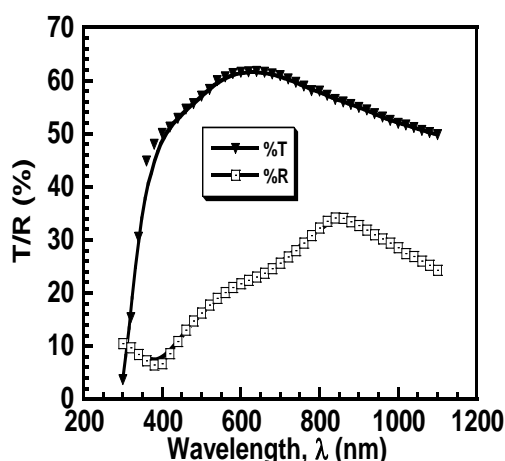
Fig. 8 Variation of transmittance/reflectance vs. wavelength for annealed Cr$_2$O$_3$ films of thickness 70 nm.

In order to determine the value of optical band gap, $(\alpha h\upsilon)^{1/n}$ vs. $(h\upsilon)$ curves have been plotted, where α indicates optical absorption co-efficient, $h\upsilon$ photon energy and n represents the nature of transition. The values of the tangents, evaluated by least mean square method, intercepting the energy axis give the values of optical band gap (E_g). From these curves it is observed that best fit is obtained for $(\alpha h\upsilon)^{1/2}$ vs. $h\upsilon$ which indicates indirect allowed transition with a band gap $E_{g=}3.30$ eV. The author's value of optical band gap does agree well with the reported value of band gap by other workers [13,15,26]. The appreciable order of transmittance coupled with the moderate value of reflectance in the entire wavelength range of Cr$_2$O$_3$ film may, therefore, be of importance of this material in energy efficient device applications.

5. Conclusions

Chromium Oxide (Cr$_2$O$_3$) thin films of thickness ranges 70 – 550 nm have been prepared onto glass substrate from Cr powder by thermal evaporation method at a pressure of about 6×10^{-4} Pa. The deposition rate is about 8.72 nm/min. X-ray diffraction (XRD) study shows that Cr$_2$O$_3$ thin films are amorphous in nature. SEM study of the samples exhibits a smooth and uniform growth on the entire surface. The elemental compositions have been estimated by EDAX method. Temperature dependence of resistivity studies in air indicate that after successive 3–4 operations of heating and cooling cycle, the material exhibits a resistivity in reversible nature in the investigated temperature range. The thickness dependence of electrical conductivity is well in conformity with Fuchs–Sondheimer size effect theory. The Hall studies reveal that both the as-deposited and annealed films are of p-type semiconductor. The carrier concentration of the samples is found in the range of 2.55×10^{26} to 3.57×10^{26} m^{-3} at room temperature. Thermoelectric power study of Cr$_2$O$_3$ samples exhibits a p-type carrier. Optical studies exhibit an appreciable order of transmittance in the visible as well as in the near infra-red

region. Author's study of band gap determination from the optical data does agree well with the value of band gap by other workers. The appreciable order of transmittance coupled with the moderate value of reflectance in the entire wavelength range of Cr$_2$O$_3$ film may, therefore, be of importance of this material in energy efficient device applications.

References

[1] X. Pang, K. Gao, F. Luo, H. Yang, L. Qiao, Y. Wang, A. A. Volinsky, Thin Solid Films **516**, 4685 (2008)
[2] B. Brushan, G. Theunissen, X. Li, Thin Solid Films **311**, 67 (1997)
[3] M. G. Hutchins, Surf. Tech. **20**, 301 (1983)
[4] F. Geotti-Bianchini, M. Guglielmi, P. Polato, G.D. Soraru, J. Non-crystall. Solids **63**, 251 (1984)
[5] A. P. Schuster, D. Nguyen, O. Caporaletti, Sol. Ener. Mater. **13**, 153 (1986)
[6] R. Koksbang, P. Norby, Electrochem. Acta. **36**, 727 (1991)
[7] T. Maruyama, H. Akagi, J. Electrochem. Soc. **143**, 1955 (1996)
[8] S. M. Machaggan, R. T. Kivaisi, E. M. Lushiku, Sol. Ener. Mater. **19**, 315 (1999)
[9] P. Hones, M. Diserens, F. Lévy, Surf. Coat. Tech. **120-121**, 277 (1999)
[10] I. P. Parkin, M. N. Field, J. Phys. IV France 09, Pr8-387 (1999)
[11] J. Wang, A. Gupta, T. M. Klein, Thin Solid Films **16**, 7366 (2008)
[12] C. S. Cheng, H. Gomi, H. Sakata, Phys. Stat. Sol. (a) **155**, 417 (1996)
[13] T. Ivanova, M. Surtchev, K. Gesheva, Phys. Stat. Sol. (a) **184**, 507 (2001)
[14] R. H. Misho, W. A. Murad, G. H. Fattahallah, Thin Solid Films **169**, 235 (1989)
[15] M. Tabbal, S. Kahwaji, T. C. Christidis, B. Nsouli, K. Zahraman, Thin Solid Films **515**, 1976 (2006)
[16] S. Tolansky, Multiple beam interferometry of surfaces and films, Oxford University Press, London (1948).
[17] J. S. Foord, R. M. Lambert, Surf. Sci. **169**, 327 (1986)
[18] G. Gewinner, J. C. Peruchetti, A. Jaegle, A. Kalt, Surf. Sci. **78**, 439 (1978)
[19] R. C. Ku, W. L. Winterbottom, Thin Solid Films **127**, 241 (1985)
[20] Van der Pauw, Philips Res. Rept. **13**, 1 (1958)
[21] C. A. Neugebauer, G. Hass, R. E. Thun, Physics of thin films **2**, 1 (1970)

[22] K. Fuchs, Pro. Cambridge Phil. Soc. **34**, 100 (1938)
[23] F. H. Sondheimer, Phys. Rev. **80**, 401 (1950)
[24] C. Kittel, Introduction to Solid State Physics, John Wiley and Sons Inc., Singapore (1995)
[25] V. D. Das, J. C. Mohanty, J. Appl. Phys. **54**, 977 (1983)

[26] E. Jacobsohn, J. Zahavi, A. Rosen, S. Nadiv, J. Mat. Sci. **26**, 1861 (1991)

_____
*Corresponding author: kakhan_ru@yahoo.ca,
                       jnain.apee@ru.ac.bd